

Electronic Supporting Information

“Induced-Fit Suction” effect: A Booster for Biofuel Storage and Separation

He Li^{†, a}, Fangyuan Guo^{†, b}, Jun Hu^{, a}, Changjun Peng^a, Hualin Wang^b, Honglai Liu^{*, a}, Jing Li^{*, c}*

^aState Key Laboratory of Chemical Engineering and School of Chemistry and Molecular Engineering, East China University of Science and Technology, 130 Meilong Road, Shanghai 200237, China.

^bNational Engineering Laboratory for Industrial Wastewater Treatment, East China University of Science and Technology, 130 Meilong Road, Shanghai 200237, China.

^cDepartment of Chemistry and Chemical Biology, Rutgers University, 123 Bevier Road, Piscataway, NJ, 08854, United States.

E-mail: junhu@ecust.edu.cn; hlliu@ecust.edu.cn; jingli@rutgers.edu

Table of Contents

Section 1. Materials, Experimental procedures and Characterization

Section 2. Computational details

1. Calculation of n-butanol/water adsorption selectivity
2. The relationship between the uptakes of n-butanol in ZIF-7-NH₂(10) and the gate-opening pressure ($P/P_0=0.1$)

3. Adsorption of n-butanol by ZIF-7-NH₂(10) and ZIF-7 particles in 5wt% n-butanol aqueous solution4. Model construction and binding energy calculation

Section 3. Fig. S1 - Fig. S14 and Table S1- Table S3

Table S1. Parameters of n-butanol aqueous solution at different concentrations and separation selectivity.

Figure S1. The crystal structures of a) ZIF-7-NH₂ and b) ZIF-7.

Figure S2. Two possible entrances in ZIF-7-NH₂; a) perpendicular to the cage (Entrance I); and b) oblique insertion (Entrance II).

Figure S3. a) FTIR spectra and b) XRD patterns of ZIF-7 and ZIF-7-NH₂(n) with various amounts of amino-groups.

Figure S4. XRD patterns of ZIF-7 immersed in water (black), n-butanol (red), vacuum treatment at 373K for 12 h (blue), as-synthesized (orange).

Figure S5. Solution 1H NMR: a)ZIF-7; b) ZIF-7-NH₂(10); c) ZIF-7-NH₂(30); d) ZIF-7-NH₂(50).

Table S2 Comparison of the content of 2-aminobenzimidazole in ZIF-7-NH₂(x) by digesting the samples in the acetic acid-d₄ solution

Figure S6. FESEM images of a) ZIF-7; b) ZIF-7-NH₂; and TEM images of c) ZIF-7; d) ZIF-7-NH₂.

Figure S7. Comparison of adsorption performance of n-butanol (●and○) and water (●and○) in ZIF-7-NH₂(n) at 298K, respectively.

Figure S8. Selectivity of ZIF-7-NH₂(10) and ZIF-7 materials with varying n-butanol fractions.

Figure S9. N₂ adsorption isotherm of ZIF-7-NH₂ and ZIF-7 at 77K.

Figure S10. Binding energies of n-butanol molecule with ZIF-7-NH₂ cage and the induced structure deformations at five different stages in the simulated adsorption process (A) approaching the cage, (B) at the gate of entrance, (C) inside the cage, (D) at the opposite-side gate of the cage, and (E) leaving the cage.

Figure S11. Binding energies of n-butanol or water molecules with ZIF-7-NH₂ or ZIF-7 cages and their induced structure deformations: a) n-butanol molecule at the surface of the cage; b) n-butanol molecule inside the cage; c) water molecule at the surface of the cage; d) water molecule inside the cage.

Figure S12. Adsorption-desorption isotherms of ethanol, methanol, n-butanol and water at 298 K in ZIF-7-NH₂(30).

Figure S13. Binding energies of water, n-butanol, ethanol and methanol molecules with the cage of ZIF-7-NH₂ at five different stages in the simulated adsorption process (A) approaching the cage, (B) at the gate of entrance, (C) inside the cage, (D) at the opposite-side gate of the cage, and (E) leaving the cage

Figure S14. Induce structure deformations of ZIF-7-NH₂ cage by ethanol, methanol, n-butane, and water molecules at five different stages in the simulated adsorption process (A) approaching the cage, (B) at the gate of entrance, (C) inside the cage, (D) at the opposite-side gate of the cage, and (E) leaving the cage.

Table S3 Comparison of experimental results for n-butanol adsorption in different samples.

Section 4. References

Section 1.

Materials

Benzimidazole (BzIM, 98%) and 2-aminobenzimidazole (2-amBzIM, 97%) were purchased from Adamas-beta. Zinc nitrate hexahydrate, Methanol (99.9%), N,N-dimethylformamide (DMF, 99.99%) were purchased from Shanghai TiTan Scientific Co., Ltd. All the chemicals were used as received without further purification.

Experimental Procedures

ZIF-7 and ZIF-7-NH₂ particles synthesis

ZIF-7 was prepared according to the preparation method of Tu et al.¹ and ZIF-7-NH₂ was prepared according to the preparation method of Xiang et al.². Specifically, the precursor solution A was prepared by adding 10 mmol benzimidazole into 50 mL methanol, and the precursor solution B was prepared by adding 5 mmol Zn(NO₃)₂·6H₂O into 50 mL DMF, respectively. Then, Precursor A and B were poured into a 100 mL beaker, simultaneously. Under stirring, the mixture slowly became turbid, and after stirring about 30 min, the as-synthesized ZIF-7 was collected by centrifugation (7800 rpm, 1.5 h).

For preparing nanoparticles of ZIF-7-NH₂, the mixed precursor solution C was prepared by adding total 10 mmol benzimidazole and 2-aminobenzimidazole with different molar ratios of x:y into 50 mL methanol. After completely dissolving, precursor C and precursor B were poured into a 100 mL beaker simultaneously and were stirred for 6h at room temperature (298 K). This was then followed by centrifugation (10000 rpm, 15 min) and washing with methanol for three times. Finally, the as-synthesized ZIF-7-NH₂(n) (n=y/(x+y)) precipitates were dried at 353K for 12 h.

Characterization

Fourier transform infrared spectroscopy (FTIR) was employed by using a NEXUS 470 (Thermo Nicolet) with a scan range from 400 to 4000 cm⁻¹. The powder crystal structure ZIF-7 and ZIF-7-NH₂ were analyzed by Rotating Anode X-ray Powder Diffractometer, 18KW/D/max2550VB/PC (Copper Target 18KW(450mA), Programmed Variable Slit System, Fully Automated Curved (Plate) Crystal Graphite Monochromator, JADE 5.0Software, Anton Paar XRK-900 High Temperature in-situ Reactor, the range of 2θ=5°-35°, at a step of 0.02°). To determine the content of the amino in the mix-ligand ZIF-7-NH₂(x), all samples were analyzed with solution ¹H NMR spectroscopy on a Ascend 600 MHz spectrometer after digesting samples using d₄-acetic acid. Prior to digesting in the deuterium solvent, all samples were processed by the soxhlet extraction(methanol) to remove other occluded ligands, followed by the vacuum drying at 150°C for 12h. The morphology of ZIF-7 and ZIF-7-NH₂ were analyzed with a field emission scanning electron microscope (FESEM), S-3400N (HITACHIJapan). The porous property of ZIF-7 and ZIF-7NH₂ were analyzed with high resolution transmission electron microscopy (HRTEM), JEM-2100 (Japan). The surface area, N₂ adsorption(liquid nitrogen bath) of ZIF-7 and ZIF-7-NH₂ were all collected on Micrometrics tristar II. Each sample was degassed for 8 h at 373K before analysis. The adsorption-desorption isotherms of butanol, ethanol, methanol were analyzed by Hiden IGA-100B (intelligent gravitation analyzer-100B), Each sample was degassed for 8 h at 373K before analysis (Balance capacity: 1g; Range: 200 mg; (standard) Accuracy: 0.1 μg; Pressure range: UHV~20bar; Pressure resolution: 1/16000 of range ; Accuracy: ±0.02% of range; Measurement range: 77K~773K; Resolution: ±263K (Type K)).

Section 2.

Computational details

1. n-butanol/water selectivity (S) was calculated by the ideal adsorption solution theory³ (IAST) as Eq. 1. The partial pressure at equilibrium was calculated by the Raoult's law as Eq. 2. To make more accurate, the activity coefficient was introduced, which was calculated by Non-Random Two Liquid (NRTL) method in Aspen Plus[®].

$$S = \frac{q_i/p_i}{q_j/p_j} \quad (\text{Equation 1})$$

$$p_i = P_i^* x_i r_i \quad (\text{Equation 2})$$

$$\text{In which } x_i = \frac{w_i/M_i}{w_i/M_i + w_j/M_j} \quad (\text{Equation 3})$$

Where S is the ideal selectivity of i/j , q_i is the adsorption quantities, p_i is the partial pressure. x_i is the molar fraction, w_i is the weight, M_i is the molar mass. P_i^* is the saturated vapor pressure, r_i is the activity coefficient, the adsorption isotherm of n-butanol was fitted with Allometrix model and Logistic model in Origin 9 for ZIF-7 and ZIF-7-NH₂(10), respectively.

Table S1. Parameters of n-butanol aqueous solution at different concentrations and separation selectivity.

Concentration	1wt%	2wt%	3wt%	4wt%	5wt%
Activity coefficient (r_b)	263.1811	134.3364	87.80729	65.88479	52.31375
Activity coefficient (r_w)	1.002485	1.004901	1.00753	1.010071	1.012725
Mole fraction (x_b)	0.0025	0.0049	0.00746	0.0101	0.01263
Mole fraction (x_w)	0.9975	0.9951	0.9925	0.9899	0.9874
Partial pressure (p_b , kPa)	0.5908	0.5908	0.588	0.5916	0.5933
Partial pressure (p_w)	3.1699	3.1699	3.1699	3.1698	3.1698

kPa)					
Adsorption quantity of n-butanol in ZIF-7-NH ₂ (10) (q _b , g/g)	0.1481	0.1481	0.148	0.1481	0.1481
Adsorption quantity of water in ZIF-7-NH ₂ (10) (q _w , g/g)	0.021	0.021	0.021	0.021	0.021
Adsorption quantity of n-butanol in ZIF-7 (q _b , g/g)	0.0331	0.0331	0.033	0.0332	0.0332
Adsorption quantity of n-butanol in ZIF-7 (q _b , g/g)	0.072	0.072	0.072	0.072	0.072
ZIF-7-NH ₂ (10) Selectivity (b/w)	39.73	39.73	39.89	39.68	39.56
ZIF-7 Selectivity (b/w)	2.45	2.45	2.46	2.46	2.45

[a] The saturated vapour pressure of n-butanol and water (P^*_b and P^*_w) were 0.898kPa and 3.17kPa at 298K, respectively. [b] The abbreviations of n-butanol and water were denoted as b and w , respectively.

Taking 1wt% butanol concentration at 298K for example:

$$x_b = \frac{w_b/M_b}{w_b/M_b + w_w/M_w} = \frac{0.04/74.12}{0.04/74.12 + 0.96/18.01} = 0.0025 p_b = p_b^* * x_b^*$$

$$x_w = 1 - x_b = 1 - 0.0025 = 0.9975$$

$$p_w = p_w^* * x_w * r_w = 3.17 * 0.9975 * 1.002485 = 3.1699 kPa$$

$$\text{ZIF-7: } s_{b/w} = \frac{q_b/p_b}{q_w/p_w} = \frac{0.0331/0.5908}{0.07244/3.17} = 2.45$$

$$\text{ZIF-7-NH}_2(10): s_{b/w} = \frac{q_b/p_b}{q_w/p_w} = \frac{0.1481/0.5908}{0.021/3.17} = 39.73$$

2. The relationship between the uptakes of n-butanol in ZIF-7-NH₂(10) and the gate-opening pressure (P/P₀=0.1).

As shown below (downloaded from CCDC: <https://www.ccdc.cam.ac.uk/>), for ZIF-7-NH₂ with one amino group substitution, the molar mass of one cage is:

1 cage = 2701.581 g/mol, Then, 1g ZIF-7-NH₂=3.701×10⁻⁴ mol·cage,

The n-butanol uptake at P/P₀=0.1 is 0.356mmol/g, accordingly, the number of n-butanol per unit cage is:

$$0.35582\text{mmol}/3.701 \times 10^{-4} \text{ mol} \cdot \text{cage} = 0.96 \text{ cage}^{-1}$$

which means there was approximately one n-butanol molecule within one cage of ZIF-7-NH₂ when the sharp increase of n-butanol amount occurred. This is exactly the same as what we predicted that when a n-butanol molecule was adsorbed, it acted as the “gate-keeper” to keep the benzene ring in the open-gate conformation

3. Adsorption of n-butanol by ZIF-7-NH₂(10) and ZIF-7 particles in 5wt% n-butanol aqueous solution

Before adsorption experiments, the particles were activated at 393K by kept it for 12h in vacuum oven so as to remove impurities. Liquid phase adsorption experiments were performed in closed stirred glass bottles of 5mL. Solutions were prepared by adding appropriate amounts of n-butanol to water. Approximately 2 mL of 5 % n-butanol solution in H₂O and 100 mg particles were added to the bottle, and the suspension was allowed to achieve the absorption equilibrium at 298K in 1 atm. Thereafter, the particles were separated from the solution via centrifugation at 10,000 rpm for 15 min. The supernatants were filtered using the 0.2 um syringe filter. Then the concentrations of the adsorbates were determined by Flame Ionization Detector (FID) detection⁴.

To determine the loading of the n-butanol in the particles, a mass balance equation was used:

$$q_i = \frac{m_0(C_0 - C_i)}{m_{z,0}} \quad (\text{Equation 4})$$

Where q_i is the mass loading of n-butanol, C_0 is the initial concentration of adsorbate in the solution, C_i is the concentration of the adsorbate in the solution at equilibrium, m_0 is the initial mass of the adsorbate, $m_{z,0}$ is the initial mass of the adsorbent. The solution volume changes due to the adsorbed butanol and co-adsorbed water are neglected.

4. Model construction and computational calculation details

The crystal structure of ZIF-7 was taken from the Cambridge Crystallographic Date Centre (CCDC)⁵. To reduce the computational demand, the representative fragment of ZIF-7 was taken from the all-atom frameworks, as shown in Fig. S1. The fragment of ZIF-7-NH₂ was obtained by substituting hydrogen atom on imidazole ring by amidogen. All of the calculations in this work were carried out using the Material Studio software⁶.

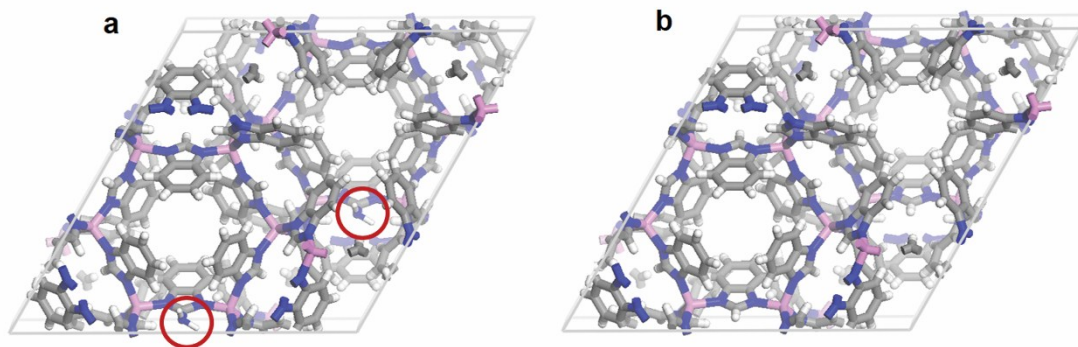


Figure S1. The crystal structures of a) ZIF-7-NH₂ and b) ZIF-7.

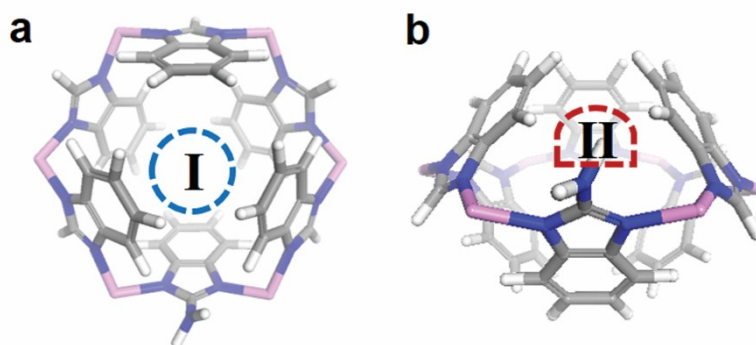


Figure S2. Two possible entrances in ZIF-7-NH₂; a) perpendicular to the cage (Entrance I); and b) oblique insertion (Entrance II).

We applied quantum calculation (QM) to investigate the binding energies of the molecules (water, n-butanol, ethanol, methanol, butane) with the cages of ZIF-7-NH₂ and ZIF-7, respectively.

$$E = E_{total} - E_{cages} - E_{molecules} \quad (\text{Equation 4})$$

Where the E is the binding energy between the cages and the molecules. E_{cages} , $E_{molecules}$, and E_{total} , are the energies of the cages, molecules and their complex, respectively. All of the structures are optimized before energy calculation. First, we used the molecular mechanics (MM) method to generate the initial structures by the Forcite module of the software, where the universal force field (UFF) was used to model the atomic interactions⁷. Second, we used density functional theory (DFT) to calculate E_{cages} , $E_{molecules}$, and E_{total} , which is performed by the Dmol3 module. The Perdew-Burke-Ernzerhof (PBE) method was used to approximate the exchange correlation energy⁸. The double-numeric basis plus polarization orbitals (DNP) was used for valence electrons. The self-consistent framework (SCF) was used to solve the Kohn-Sham equations. The SCF iteration was assumed to converge when the energy change lower than 2.57×10^{-3} kJmol⁻¹. The geometry optimization was assumed to converge when the energy change lower than 2.7×10^{-4} eV, force lower than 0.05 eV Å⁻¹, and displacement lower than 0.005 Å. The dispersion interaction via the D2 method of Grimme (DFT-D) is include in the calculations⁹.

Section 3.

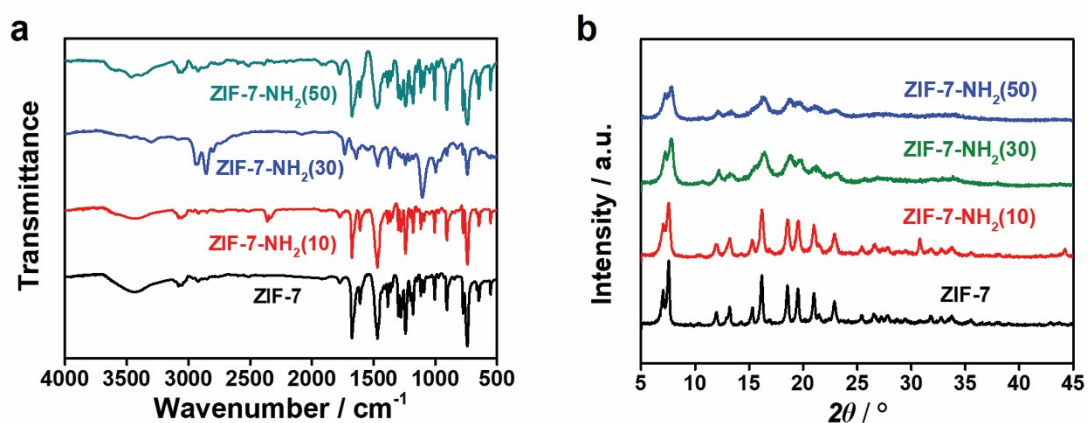


Figure S3. a) FTIR spectra and b) XRD patterns of ZIF-7 and ZIF-7-NH₂(n) with various amounts of amino-groups.

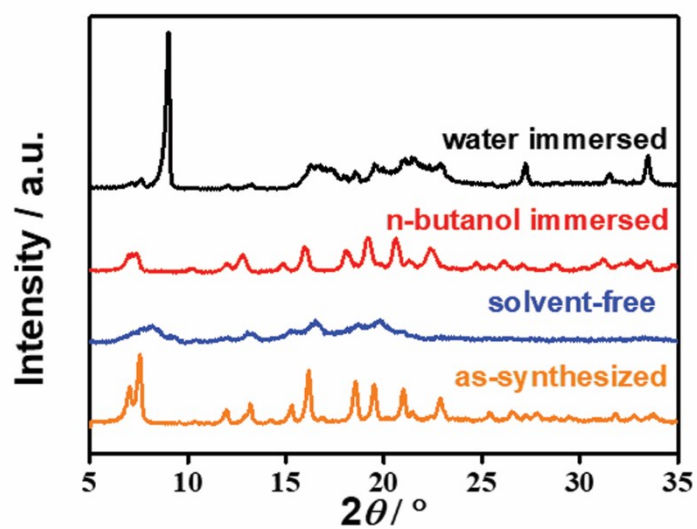


Figure S4. XRD patterns of ZIF-7 immersed in water (black), n-butanol (red), vacuum treatment at 373K for 12 h (blue), as-synthesized (orange).

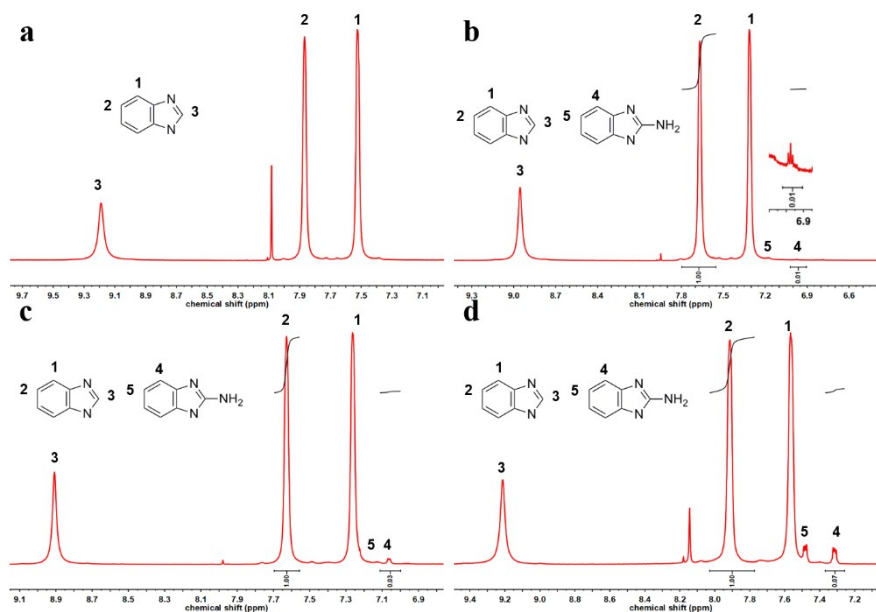


Figure S5. Solution ¹H NMR: a) ZIF-7; b) ZIF-7-NH₂(10); c) ZIF-7-NH₂(30); d) ZIF-7-NH₂(50).

Table S2. Comparison of the content of 2-aminobenzimidazole in ZIF-7-NH₂(x) by digesting the samples in the acetic acid-d₄ solution.

Samples	Theoretical content of 2-aminobenzimidazole (mol%)	Experimental content of 2-aminobenzimidazole (mol%)
ZIF-7	0	0
ZIF-7-NH ₂ (10)	10	1
ZIF-7-NH ₂ (30)	30	3
ZIF-7-NH ₂ (50)	50	7

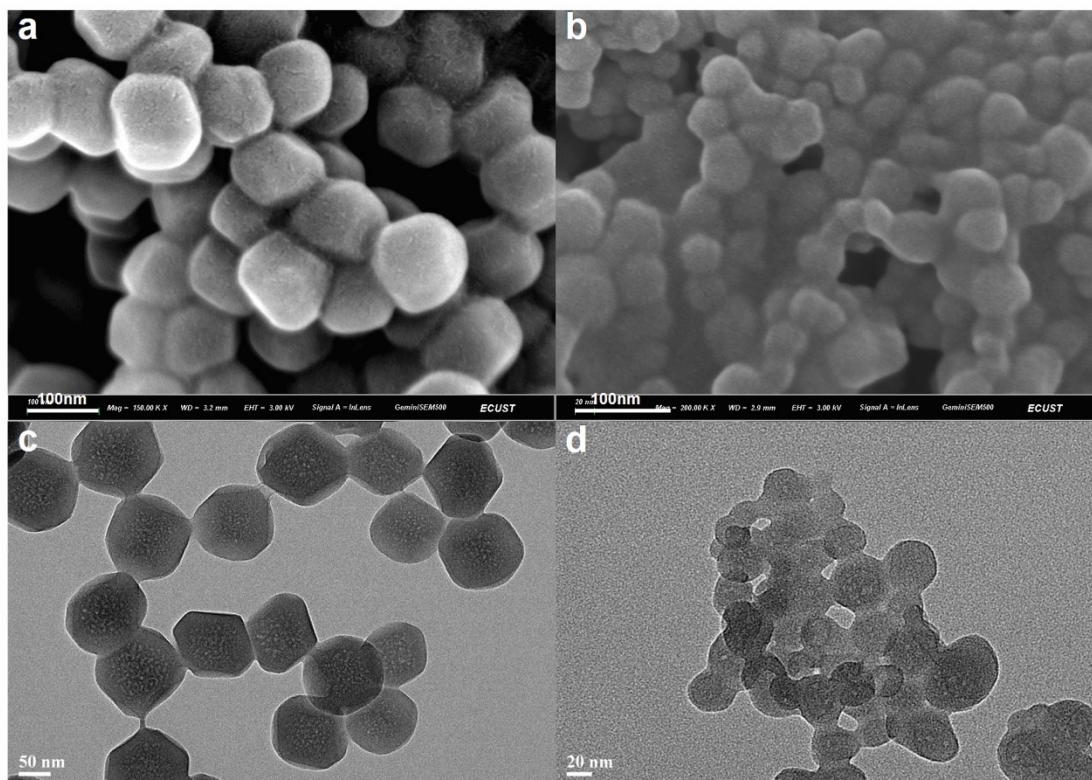


Figure S6. FESEM images of a) ZIF-7; b) ZIF-7-NH₂; and TEM images of c) ZIF-7; d) ZIF-7-NH₂.

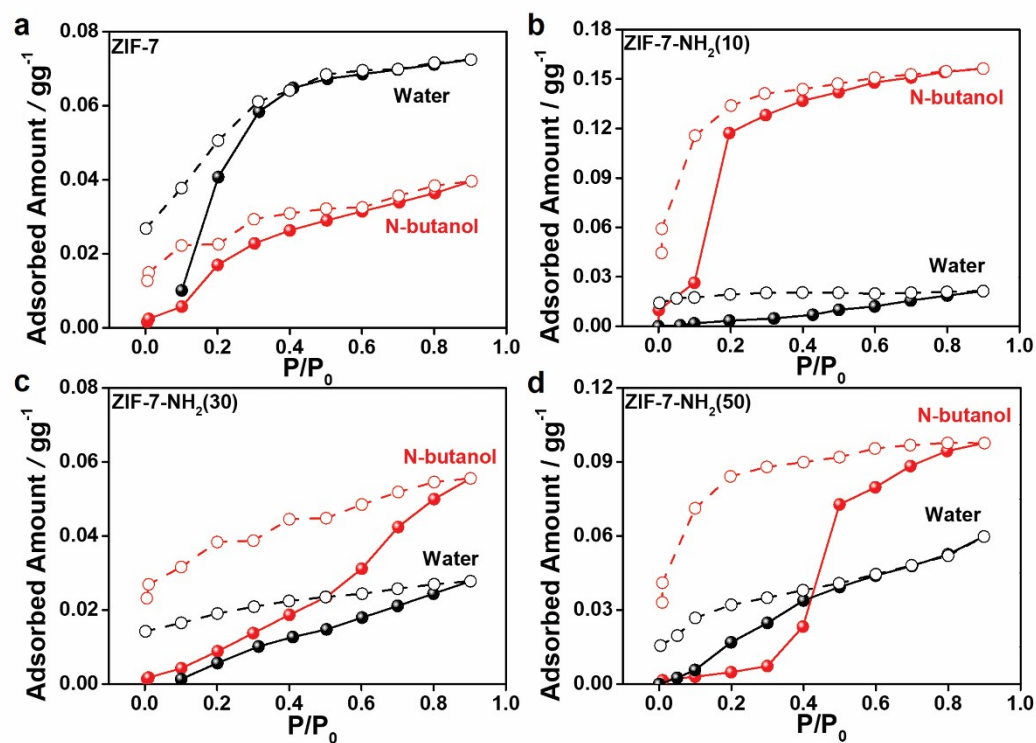


Figure S7. Comparison of adsorption performance of n-butanol (●and○) and water (●and○) in ZIF-7-NH₂(n) at 298K, respectively.

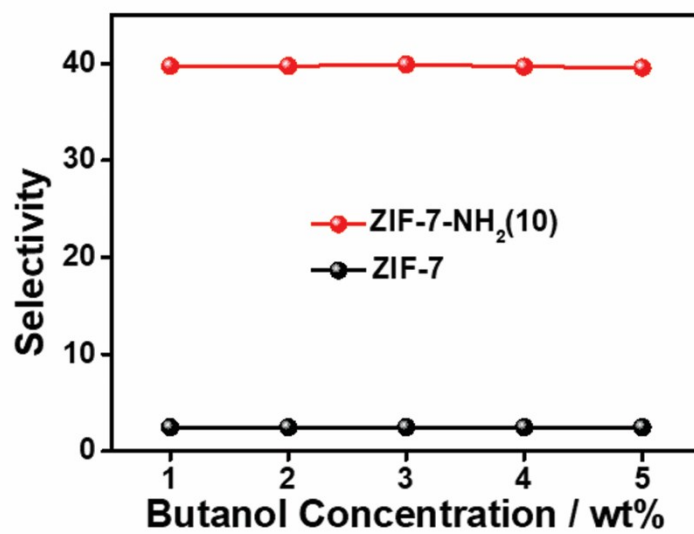


Figure S8. Selectivity of ZIF-7-NH₂(10) and ZIF-7 materials with varying n-butanol fractions.

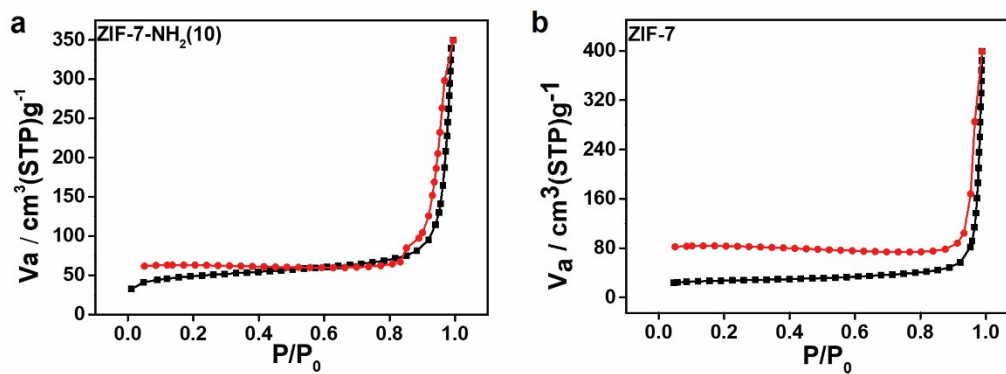


Figure S9. N₂ adsorption isotherm of ZIF-7-NH₂ and ZIF-7 at 77K.

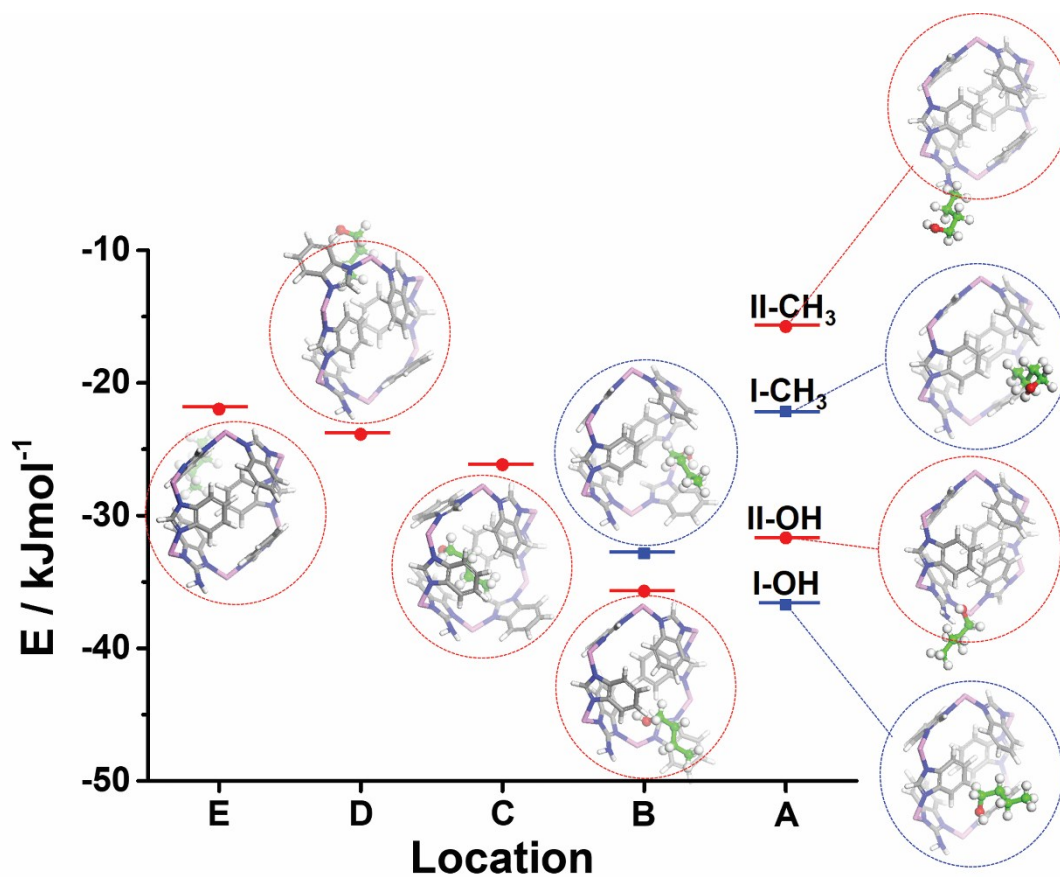


Figure S10. Binding energies of n-butanol molecule with ZIF-7-NH₂ cage and the induced structure deformations at five different stages in the simulated adsorption process (A) approaching the cage, (B) at the gate of the cage, (C) inside the cage, (D) at the opposite-side gate of the cage, and (E) leaving the cage.

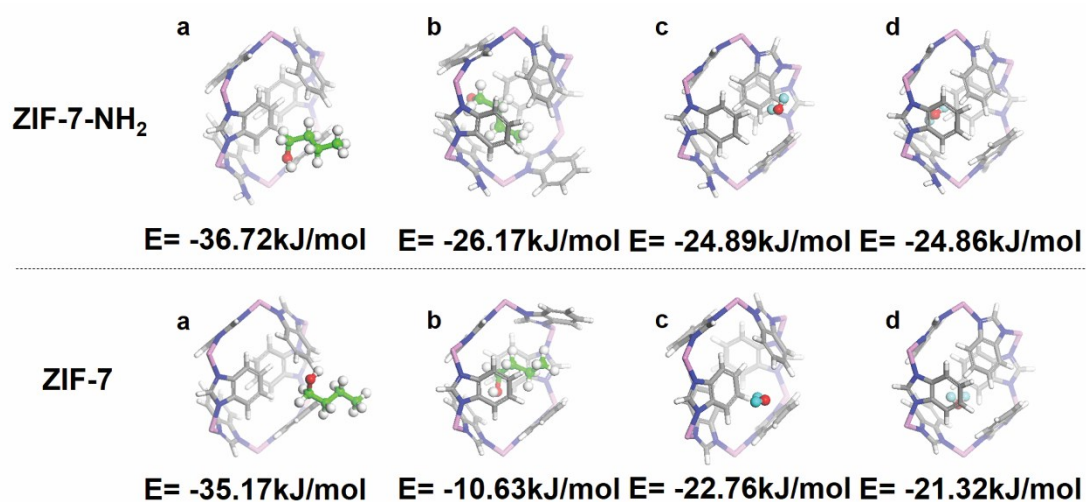


Figure S11. Binding energies of n-butanol or water molecules with ZIF-7-NH₂ or ZIF-7 cages and their induced structure deformations: a) n-butanol molecule at the surface of the cage; b) n-butanol molecule inside the cage; c) water molecule at the surface of the cage; d) water molecule inside the cage.

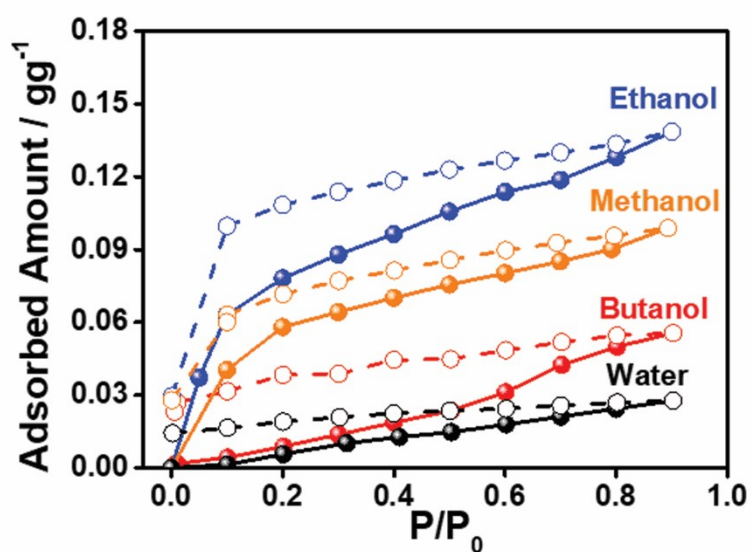


Figure S12. Adsorption-desorption isotherms of ethanol, methanol, n-butanol and water at 298 K in ZIF-7-NH₂(30).

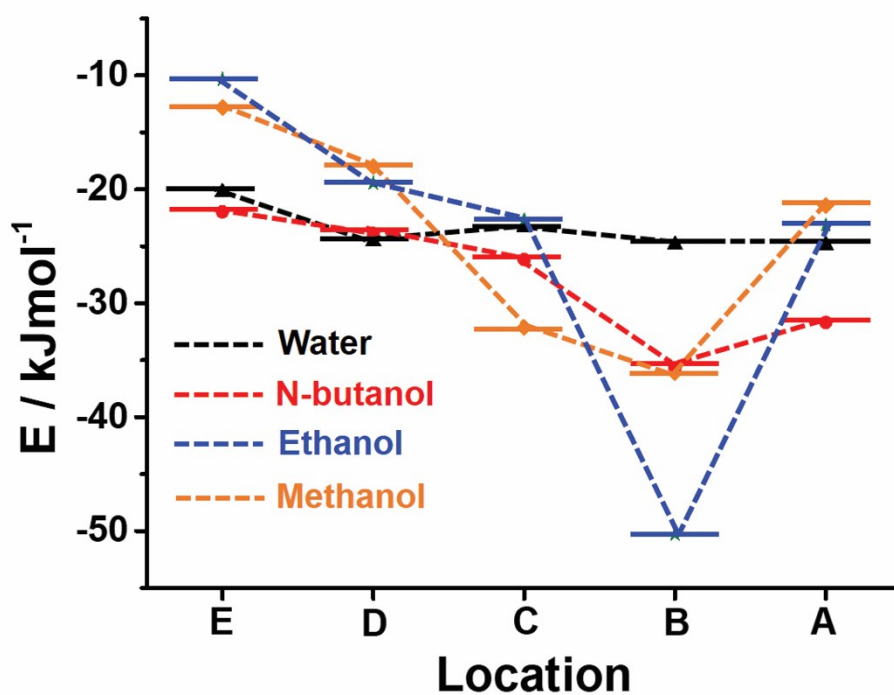


Figure S13. Binding energies of water, n-butanol, ethanol and methanol molecules with the cage of ZIF-7-NH₂ at five different stages in the simulated adsorption process: (A) approaching the cage, (B) at the gate of the cage, (C) inside the cage, (D) at the opposite-side gate of the cage, and (E) leaving the cage.

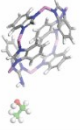
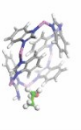
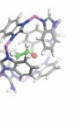
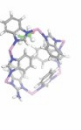
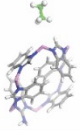

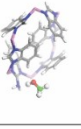
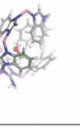
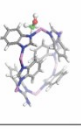
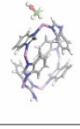
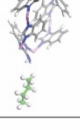
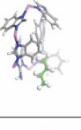
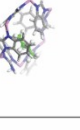
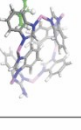
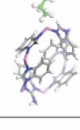
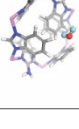
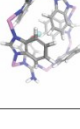
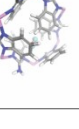
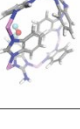
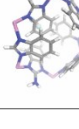
	A		B		C		D		E	
	Structure	E(kJ/mol)	Structure	E(kJ/mol)	Structure	E(kJ/mol)	Structure	E(kJ/mol)	Structure	E(kJ/mol)
ETOH		-23.14		-50.28		-22.69		-19.45		-10.35
MEOH		-21.41		-36.09		-32.13		-17.98		-12.81
n-Butane		-17.00		-14.18		-39.96		-22.59		-24.08
Water		-24.89		-24.86		-23.32		-24.55		-20.24

Figure S14. Induced structure deformations of the ZIF-7-NH₂ cage by ethanol, methanol, n-butane, and water molecules at five different stages in the simulated adsorption process (A) approaching the cage, (B) at the gate of the cage, (C) inside the cage, (D) at the opposite-side gate of the cage, and (E) leaving the cage.

Table S3. Comparison of experimental results for n-butanol adsorption in different samples.

Samples	Method of adjusting amphiphilicity	BET surface areas (m ² /g)	N-butanol concentration	Temperature (K)	N-butanol uptake (mmol/g)	Ref.
ZIF-8 ₇₀ -90 ₃₀	Mixed ligands (2-Methylimidazole and 4,5-dichloroimidazole)	1310	11%	308	4	10
MFI and CHA crystal	zeolite crystals on hydrophilic substrates	442	2%		1.75/2.43	4
PC750	Pyrolysis	502.38	2.5-25g/L	298	2.02	11
Calix[n]arenes/SiO ₂	Calixarenes grafted on hydrophilic SiO ₂ surface	500	0-0.2mol/L	293	0.12	12
ZIF-7-NH ₂ (10)	Mixed ligands (2-aminobenzimidazole and Benzimidazole)	70.4	5%	298	4.33	This work

Section 4.

References

- 1 Tu, M.; Wiktor, C.; Rosler, C.; Fischer, R. A. *Chemical communications*, 2014, **50**, 13258.
- 2 Xiang, L.; Sheng, L.; Wang, C.; Zhang, L.; Pan, Y.; Li, Y. *Advanced materials*, 2017, **29**.
- 3 Walton, K. S.; Sholl, D. S. *AIChE Journal*, 2015, **61**, 2757.
- 4 Ming Zhou and Jonas Hedlund. *Angewandte Chemie*, 2018, **57**, 10966.
- 5 <https://www.ccdc.cam.ac.uk/>
- 6 Andzelm, J.; King-Smith, R.; Fitzgerald, G. *Chemical physics letters*, 2001, **335**, 321.
- 7 Rappe, A.; Colwell, K.; Casewit, C. *Inorganic chemistry*, 1993, **32**, 3438.
- 8 Perdew, J. P.; Burke, K.; Ernzerhof, M. *Physical review letters*, 1996, **77**, 3865.
- 9 Grimme, S.; Antony, J.; Ehrlich, S.; Krieg, H. *The Journal of chemical physics*, 2010, **132**, 154104.
- 10 Bhattacharyya, S.; Jayachandrababu, K. C.; Chiang, Y.; Sholl, D. S.; Nair, S. *ACS Sustainable Chemistry & Engineering*, 2017, **5**, 9467.
- 11 Han, M.; Jiang, K.; Jiao, P.; Ji, Y.; Zhou, J.; Zhuang, W.; Chen, Y.; Liu, D.; Zhu, C.; Chen, X.; Ying, H.; Wu, J. *Scientific reports*, 2017, **7**, 11753.
- 12 Anthony B. Thompson, Sydney J. Cope, T. Dallas Swift, and Justin M. Notestein. *Langmuir*, 2011, **27**, 11990.